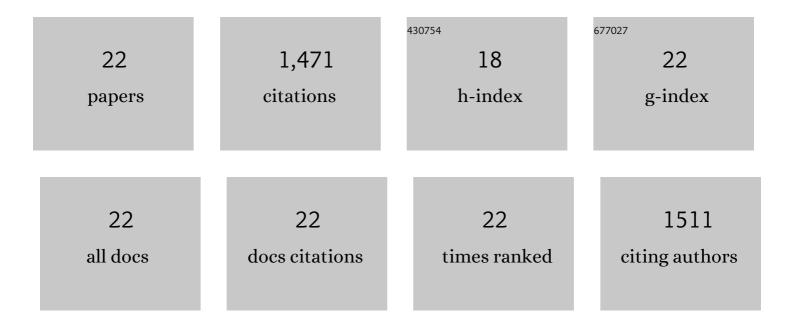
## Xiong, Cheng

List of Publications by Year in descending order

Source: https://exaly.com/author-pdf/3722542/publications.pdf Version: 2024-02-01



XIONC CHENC

#	Article	IF	CITATIONS
1	Boron phosphide monolayer as a potential anode material for alkali metal-based batteries. Journal of Materials Chemistry A, 2017, 5, 672-679.	5.2	217
2	A high power density and long cycle life vanadium redox flow battery. Energy Storage Materials, 2020, 24, 529-540.	9.5	214
3	Copper nanoparticle-deposited graphite felt electrodes for all vanadium redox flow batteries. Applied Energy, 2016, 180, 386-391.	5.1	166
4	A high-performance carbon nanoparticle-decorated graphite felt electrode for vanadium redox flow batteries. Applied Energy, 2016, 176, 74-79.	5.1	145
5	Highly catalytic and stabilized titanium nitride nanowire array-decorated graphite felt electrodes for all vanadium redox flow batteries. Journal of Power Sources, 2017, 341, 318-326.	4.0	134
6	Highly catalytic hollow Ti3C2Tx MXene spheres decorated graphite felt electrode for vanadium redox flow batteries. Energy Storage Materials, 2020, 25, 885-892.	9.5	87
7	Highly active, bi-functional and metal-free B 4 C-nanoparticle-modified graphite felt electrodes for vanadium redox flow batteries. Journal of Power Sources, 2017, 365, 34-42.	4.0	75
8	2D Ti <sub>3</sub> C <sub>2</sub> T <sub>x</sub> MXenes: Visible Black but Infrared White Materials. Advanced Materials, 2021, 33, e2103054.	11.1	72
9	Achieving multiplexed functionality in a hierarchical MXene-based sulfur host for high-rate, high-loading lithium-sulfur batteries. Energy Storage Materials, 2020, 33, 147-157.	9.5	64
10	Remedies of capacity fading in room-temperature sodium-sulfur batteries. Journal of Power Sources, 2018, 396, 304-313.	4.0	45
11	Enhanced cycle life of vanadium redox flow battery via a capacity and energy efficiency recovery method. Journal of Power Sources, 2020, 478, 228725.	4.0	33
12	Bifunctional effect of laser-induced nucleation-preferable microchannels and <i>in situ</i> formed LiF SEI in MXenes for stable lithium-metal batteries. Journal of Materials Chemistry A, 2020, 8, 14114-14125.	5.2	33
13	A high-performance ethanol–hydrogen peroxide fuel cell. RSC Advances, 2014, 4, 65031-65034.	1.7	32
14	A composite solid electrolyte with an asymmetric ceramic framework for dendrite-free all-solid-state Li metal batteries. Journal of Materials Chemistry A, 2021, 9, 9665-9674.	5.2	30
15	Honeycombâ€like hierarchical porous silicon composites with dual protection for ultrastable Liâ€ionÂbattery anodes. SmartMat, 2021, 2, 579-590.	6.4	21
16	Mn <sub>3</sub> O <sub>4</sub> Nanoparticleâ€Decorated Carbon Cloths with Superior Catalytic Activity for the V <sup>II</sup> /V <sup>III</sup> Redox Reaction in Vanadium Redox Flow Batteries. Energy Technology, 2018, 6, 1228-1236.	1.8	20
17	Mathematical modeling of the charging process of Li-S batteries by incorporating the size-dependent Li2S dissolution. Electrochimica Acta, 2019, 296, 954-963.	2.6	20
18	Artificial Bifunctional Protective layer Composed of Carbon Nitride Nanosheets for High Performance Lithium–Sulfur Batteries. Journal of Energy Storage, 2019, 26, 101006.	3.9	19

Xiong, Cheng

#	Article	IF	CITATIONS
19	A safe and efficient lithiated silicon-sulfur battery enabled by a bi-functional composite interlayer. Energy Storage Materials, 2020, 25, 217-223.	9.5	19
20	On-Site Fluorination for Enhancing Utilization of Lithium in a Lithium–Sulfur Full Battery. ACS Applied Materials & Interfaces, 2020, 12, 53860-53868.	4.0	12
21	An <i>in situ</i> encapsulation approach for polysulfide retention in lithium–sulfur batteries. Journal of Materials Chemistry A, 2020, 8, 6902-6907.	5.2	9
22	A Li <sub>2</sub> Sâ€Based Sacrificial Layer for Stable Operation of Lithiumâ€Sulfur Batteries. Energy Technology, 2018, 6, 2210-2219.	1.8	4